AD_____

Award Number: DAMD17-02-1-0198

TITLE: Molecular Pathogenesis of Rickettsioses and Development of Novel Anti-Rickettsial Treatment by Combinatorial Peptide-Based Libraries

PRINCIPAL INVESTIGATOR: David H. Walker, M.D.

CONTRACTING ORGANIZATION: University of Texas Medical School
Galveston, Texas 77555-0657

REPORT DATE: February 2003

TYPE OF REPORT: Annual

PREPARED FOR: U.S. Army Medical Research and Materiel Command
Fort Detrick, Maryland 21702-5012

REPORT DOCUMENTATION PAGE

Form Approved
OMB No. 074-0188

1. AGENCY USE ONLY (Leave blank)	2. REPORT DATE	3. REPORT TYPE AND DATES COVERED
	February 2003	Annual (1 Feb 02 - 31 Jan 03)

4. TITLE AND SUBTITLE
Molecular Pathogenesis of Rickettsioses and Development of Novel Anti-Rickettsial Treatment by Combinatorial Peptide-Based Libraries

5. FUNDING NUMBERS
DAMD17-02-1-0198

6. AUTHOR(S):
David H. Walker, M.D.

7. PERFORMING ORGANIZATION NAME(S) AND ADDRESS(ES)
University of Texas Medical School
Galveston, Texas 77555-0657

E-Mail:
dhwalker@utmb.edu

8. PERFORMING ORGANIZATION REPORT NUMBER

9. SPONSORING / MONITORING AGENCY NAME(S) AND ADDRESS(ES)
U.S. Army Medical Research and Materiel Command
Fort Detrick, Maryland 21702-5012

10. SPONSORING / MONITORING AGENCY REPORT NUMBER

11. SUPPLEMENTARY NOTES
Original contains color plates: All DTIC reproductions will be in black and white.

12a. DISTRIBUTION / AVAILABILITY STATEMENT
Approved for Public Release; Distribution Unlimited

12b. DISTRIBUTION CODE

13. Abstract ***(Maximum 200 Words)*** *(abstract should contain no proprietary or confidential information)*

The purpose of this study is to utilize adaptein libraries coded within pantropic retroviral vectors that confer protection against rickettsial pathogens and to study the molecular pathogenesis of rickettsioses. The following specific aims were proposed: 1) To establish heterogeneous cell populations, with each cell expressing a unique member of a complex combinatorial peptide-based (e.g. adaptein) library and challenge with *R. prowazekii*, *R. rickettsii*, and *O. tsutsugamushi*; 2) To determine the role of NF-κB, cytokines (TNF-α, IFN-γ, RANTES), ROS and NO in intracellular killing of rickettsia-infected monolayers containing adapteins and 3) To characterize signal transduction pathways modulating the cytoskeletal events responsible for the increased vascular permeability. During the first year of this project we were able to construct two dozen libraries encoding combinatorial 6-mer, 12-mer, and 18-mer peptides. We successfully produced these libraries in bacterial cells and transfected two different cell lines with recombinant retroviruses containing the libraries with high efficiency for rickettsial challenges. We have also developed in vitro models of endothelial barrier using rat derived microvascular endothelial cells. Measurements of endothelial permeability using FITC-dextrans in transwell settings and using ECIS have been performed. Elevation of intracellular calcium in infected cell monolayers and activation of calmodulin have also been demonstrated.

14. SUBJECT TERMS:
rickettsiae, *Orientia*, adapteins, scrub, epidemic typhus

15. NUMBER OF PAGES
31

16. PRICE CODE

17. SECURITY CLASSIFICATION OF REPORT	18. SECURITY CLASSIFICATION OF THIS PAGE	19. SECURITY CLASSIFICATION OF ABSTRACT	20. LIMITATION OF ABSTRACT
Unclassified	Unclassified	Unclassified	Unlimited

Table of Contents

I. INTRODUCTION

Rickettsiae are obligately intracellular organisms that have evolved in close association with an arthropod host. Diseases caused by these organisms are still prevalent in many parts of the world and include Rocky Mountain spotted fever (the most common rickettsiosis in the US), epidemic and endemic typhus (1-4). The latter two are still responsible for thousands of deaths around the world every year. Rickettsial diseases are found in every continent except for Antarctica and are considered both emerging and re-emerging infectious diseases. In addition, *Rickettsia prowazekii* and *R. rickettsii* are listed in the Select Agents Act and are part of the Centers for Disease Control and Prevention (CDC) and NIH category B agents and the North Atlantic Treaty Organization (NATO) select agent list for their potential use as bioterrorist/biowarfare agents (5-8). The most feared complications of rickettsial infections are the development of severe cerebral and pulmonary edema leading to permanent neurologic sequelae or death owing to respiratory failure (3-4). The target cell of rickettsial pathogens is the endothelium lining the vessels of the microvasculature, as demonstrated by studies performed on autopsy cases dying of rickettsioses and animal models (9-10). The purpose of this study is to utilize adaptein libraries coded within pantropic retroviral vectors that confer protection against rickettsial pathogens. In addition, molecular pathogenesis of rickettsioses is being studied by developing *in vitro* models to study endothelial permeability and intracellular rickettsial killing in both wild type and adaptein protected cells. The long term objective of this proposal is to develop new treatments for rickettsioses and to identify novel molecular targets of rickettsial pathogenesis that would provide sites for new therapeutic interventions, and to eventually use these targets to develop effective and rapid BWT countermeasures. The new therapeutic interventions are justified due to the narrow range of antimicrobial agents available for rickettsiae and *Orientia,* emergence of chloramphenicol- and tetracycline-resistant strains of *Orientia,* and the possibility of genetically engineered resistance.

II. RESEARCH PROGRESS

The initial months of the project were dedicated to producing large stocks of *Rickettsia prowazekii, R. rickettsii* and *Orientia tsutsugamushi*. The first two were propagated in embryonated eggs followed by dissection of the yolk sac. Each stock was quantified by plaque assays and the average titer was ~10^7 - 10^8 pfu/ml. In addition, samples of each rickettsial stock were inoculated in agar plates to assure contamination-free products. *Orientia tsutsugamushi*, Karp strain, was propagated in Vero cells and quantified by plaque assays. Large stocks were also propagated in Vero cell monolayers, and rickettsiae were subsequently renografin-purified, frozen at -80°F and quantified by plaque assays. The average number of pfu/ml was ~10^9 - 10^{10}.

A. Specific aim #1: To utilize retrovirally encoded adapteins to generate cell monolayers resistant to rickettsial challenge.

Generation of combinatorial adaptein libraries

Overview. The first year of this project was devoted to successfully developing the novel reagents required for this work. Reagents were developed on schedule. These include approximately two dozen different combinatorial protein libraries with diversities of ~10^7 - 10^8. These libraries are encoded within, and delivered by, either recombinant retroviruses or episomal plasmids.

Combinatorial adaptein libraries. Approximately two dozen libraries have been constructed in our packaging plasmid ptatCCDlib-β-gal (Fig. 1) using a half-duplex based cloning strategy. These libraries encode combinatorial 6-mer, 12-mer and 18-mer peptides, in the context of a loop region of the capsid protein. The diversity of each library ranges between $2x10^7$ to $2x10^8$. In addition, we are improving our cloning protocol to attempt to generate libraries with a diversity of $\sim10^9$.

We have modified and optimized our retroviral packaging plasmid to achieve high levels of protein expression in 293 packaging cell lines. In addition, this optimized packaging plasmid encodes for β-galactosidase to allow rapid identification and quantification of infection efficiency. This packaging plasmid generates recombinant tat-CCD retroviruses with titers $\sim10^7$ pfu/ml. Cell infected with our recombinant tat-CCD retroviruses show high levels of tat-CCD expression.

Calculation of combinatorial library diversity. Diversity of the constructed combinatorial library was calculated as the product of the overall transformation efficiency (calculated by cfu observed after plating onto culture plates) and the total plasmid DNA used for initiating library construction.

Representative observed combinatorial library diversity. For each library, the targeted diversity level was $\sim1 \times 10^8$ different sequences.
18-mer-oligonucleotide library (encoding a 6 amino acid insert with the CCD protein)
Observed library size (diversity): $\sim5 \times 10^7$
Theoretical diversity: 1×10^9 oligos, 6.4×10^7 peptides

36-mer-oligonucleotide library (encoding a 12 amino acid insert with the CCD protein)
Observed library size (diversity): $\sim2 \times 10^8$
Theoretical diversity: 1×10^{18} oligos, 4.1×10^{15} peptides

54-mer-oligonucleotide library (encoding a 18 amino acid insert with the CCD protein)
Observed library size (diversity): $\sim5 \times 10^7$
Theoretical diversity: 1×10^{27} oligos, 2.6×10^{23} peptides

Calculation of combinatorial library randomness. To determine library randomness, numerous individual colonies were sequenced from each constructed library and the observed oligonucleotide frequency compared to the expected nucleotide composition.

Representative observed combinatorial library randomness for a non-targeted 18-mer oligonucleotide. The term non-targeted indicates that the codon compositions were not specified in order to encode a specific amino acid frequency. The desired oligonucleotide usage for the non-targeted library was *NNKNNKNNKNNKNNKNNK*, where N={25% A, 25% T, 25% C, 25% G} and K={50% T, 50% G}. Theoretically, this codon frequency would encode all naturally occurring amino acids and a stop codon, with predicted amino acid frequencies of 1/32 for Asn, Asp, Cys, Gln, Glu, His, Ile, Lys, Met, Phe, Trp, Tyr, and the stop codon, 2/32 for Ala, Gly, Pro, Thr, and Val, and 3/32 for Arg, Leu, and Ser residues. Thus, for a 6-mer amino acid insert, full-length sequences would comprise approximately $(31/32)^n$ or 83% of the resulting library.

Twenty six 18-mer combinatorial library plasmids were sequenced. As expected, each sequence was unique. Representative sequences are shown below (bold face nucleotides correspond to the flanking restriction sites, underlined nucleotides correspond to the fixed Ser/Gly flanking sequences).

1: **GGATCC**TCCGGTGGTGGGTTTGTTCAGGCTGAGGGTGGTTCC**CTCGAG**
2: **GGATCC**TCCGGTGGTCGTGATGCTTCTGATTCTGGTGGTTCC**CTCGAG**

3: **GGATCC**TCCGGTGGTAAGCTTTCGCCTCATGATGGTGGTTCC**CTCGAG**
4: **GGATCC**TCCGGTGGTAATCTTTTGAGTCTTCCTGGTGGTTCC**CTCGAG**

The observed codon nucleotide frequency for the combinatorial region of 26 sequences was calculated and is summarized below.

	N	N	K
A	13%	21%	1%
T	29%	29%	56%
C	30%	30%	3%
G	28%	20%	40%

Unexpectedly, a bias against G in the third nucleotide position of the codon and against A in the first position of the codon was observed. Similar bias, although to a lesser extent, were observed in several other non-targeted libraries, and may reflect an inherent bias in the E. coli propagation of plasmids.

Representative observed combinatorial library randomness for a targeted 18-mer oligonucleotide. The term targeted indicates that the codon compositions were specified in order to encode a specific amino acid frequency or distribution (e.g., predominantly charged residues, equimolar amino acid representation). We have taken advantage of the numerous theoretical approaches used to calculate the oligonucleotide composition required to encode a desired probability distribution for amino acid. In particular, work by Peter Kim and coworkers (http://gaiberg.wi.mit.edu/cgi-bin/CombinatorialCodons) have been useful in deciding the oligonucleotide composition to employ in order to generate an equimolar amino acid composition of the insert combinatorial sequence. The theoretical oligonucleotide usage for an equimolar targeted 6-mer residue (18-mer oligonucleotide) library was $(XYZ)_6$, where X={32% A, 8% T, 21% C, 39% G}, Y={28% A, 24% T, 25% C, 23% G} and Z={60% T, 40% G}. Combinatorial library plasmids were sequenced from several targeted 6-mer peptide insert libraries. As expected, each sequence was unique. Representative sequences for two different libraries are shown below:

Representative sequences from library A1, a targeted 18-mer oligonucleotide combinatorial library (bold face nucleotides correspond to the flanking restriction sites, underlined nucleotides correspond to the fixed Ser/Gly flanking sequences).

1: **GGATCC**TCCGGTGGTGTGGATATTCGGGGTCATGGTGGTTCC**CTCGAG**
2: **GGATCC**TCCGGTGGTGCTGGGAGGAATGTTATGGGTGGTTCC**CTCGAG**
3: **GGATCC**TCCGGTGGTACGACTAGTGCGGCTACGGGTGGTTCC**CTCGAG**
4: **GGATCC**TCCGGTGGTCCGTTGGAGGGTAGGCTGGGTGGTTCC**CTCGAG**
5: **GGATCC**TCCGGTGGTTCTCTTCCTTCTGCTTATGGTGGTTCC**CTCGAG**
6: **GGATCC**TCCGGTGGTGCGGATGTTGGTACTAGTGGTGGTTCC**CTCGAG**

Observed codon nucleotide distribution for library A1, a targeted 18-mer library.

	X	Y	Z
A	31	17	0
T	11	22	61
C	17	36	0
G	42	25	39

Representative sequences from library A2, a targeted 18-mer oligonucleotide combinatorial

library (bold face nucleotides correspond to the flanking restriction sites, underlined nucleotides correspond to the fixed Ser/Gly flanking sequences). Note that sequences 1 and 6 from library A2 display a two nucleotide deletion that results in a frameshift and mutation of the carboxyl terminal sequences of the CCD protein. Such deletions and resulting frameshifts have been observed in a small number of sequences.

1: **GGATCC**TCCGGTGGTGCGATGGCTCAGATTCGGTGGTTCC**CTCGAG**
2: **GGATCC**TCCGGTGGTGCTGTTAGTGATGCTCGTGGTGGTTCC**CTCGAG**
3: **GGATCC**TCCGGTGGTCATCATGATATTAGGGGTGGTGGTTCC**CTCGAG**
4: G**GATCC**TCCGGTGGTGTGAAGGCTGCGGCTATGGGTGGTTCC**CTCGAG**
5: GG**ATCC**TCCGGTGGTAATACTAATAGGTGTAATGGTGGTTCC**CTCGAG**
6: **GGATCC**TCCGGTGGTAATGTCCTACGCATCATGGTGGTTCC**CTCGAG**
7: **GGATCC**TCCGGTGGTCTGAGTAGGGTTCAGAAGGGTGGTTCC**CTCGAG**
8: **GGATCC**TCCGGTGGTAATGATAGTTGGCTTTCGGGTGGTTCC**CTCGAG**
9: GG**ATCC**TCCGGTGGTGTTCATCTTGTTACTGAGGGTGGTTCC**CTCGAG**

Observed codon nucleotide distribution for library A2, a targeted 18-mer library.

	X	Y	Z
A	38	31	0
T	7	24	69
C	19	19	0
G	36	24	31

Representative observed combinatorial library randomness for a targeted 36-mer oligonucleotide.

Representative sequences from library LC19, a targeted 36-mer oligonucleotide combinatorial library (underlined nucleotides correspond to the fixed Ser/Gly flanking sequences). For brevity, the flanking restriction site sequences (GGATCC and CTCGAG) are not shown. All combinatorial site sequences examined from this library were complete, containing 36 nucleotides.

1: TCCGGTGGTGTTGCGCAGTTTGGGCTTTGTCGTTGTGAGGTTACTGGTGGTTCC
2: TCCGGTGGTACTTGTCTTGTTAGTGTTCTTAGTGCTCAGTTTATTGGTGGTTCC
3: TCCGGTGGTCATGTGTATGAGATTATTGTTGTGCCTAGTTCTGATGGTGGTTCC
4: TCCGGTGGTACGGCGCGTGCTGTTATTAGTAAGCATTGTGCGTGTGGTGGTTCC
5: TCCGGTGGTGCTACTACTGTTGGTGATGCTGATGTTGATACTTTTGGTGGTTCC
6: TCCGGTGGTTCTGATGGTGCGCCGGTTATTGATGCTAATACTATTGGTGGTTCC
7: TCCGGTGGTATTTTTCCTATGAAGGATCGGAATGCTGATTCGCCGAGTGGTTCC
8: TCCGGTG TGCTAGGATTAATATGCCGGCTCAGACTATTGGTCCGGGTGGTTCC
9: TCCGGTGGTACGGCGCGTGCTGTTATTAGTAAGCATTGTGCGTGTGGTGGTTCC
10: TCCGGTGGTGATCTTCGTGCGGCTCGTCGTACGGCGGGTTTTAAGGGTGGTTCC

Observed codon nucleotide distribution for library LC19, a targeted 36-mer library based upon analysis of the above ten sequences.

	X		Y		Z	
	Predicted	Actual	Predicted	Actual	Predicted	Actual
A	32	28	28	21	0	0
T	8	13	24	27	60	73
C	21	19	25	31	0	0
G	39	38	23	21	40	27

Representative observed combinatorial library randomness for a targeted 54-mer oligonucleotide. Representative sequences from library LC18, a targeted 54-mer oligonucleotide combinatorial library (underlined nucleotides correspond to the fixed Ser/Gly flanking sequences). For brevity, the flanking restriction site sequences (GGATCC and CTCGAG) are not shown. All combinatorial site sequences examined from this library were complete, containing 54 nucleotides.

1: TCCGGTGGTTAGGTTGTTCATATTCATAGTGGTCCTCATGTTGTTGGTATTGGTAATTGTGGTGGTGGTTCC
2: TCCGGTGGTCTGGCTACTTAGGCGATTCATCTTATGGGTGGTTTTTCTCGTTCTTGTGCTATTGGTGGTTCC
3: TCCGGTGGTGAGCGGATGCATGCTCCTTCTGTGCTTAATTGTTTTCTTGCTCTTTATCTGGCTAGTGGTTCC
4: TCCGGTGGTGCTACGGATACTAGGGTTGCGAATAATCCTATTACTTAGCAGCCTACTTTTGAGGGTGGTTCC
5: TCCGGTGGTGTGATGATTGCTGATCAGATTGCTCGTGCGCCTAGTGGTCCGAAGGCTCGGGTTGGTGGTTCC
6: TCCGGTGGTCTGATTAATGCTGGTGCTACGGATGTGAGTATGCTTCATGTTGAGCATAGTCCTGGTGGTTCC
7: TCCGGTGGTACTAGGGCGGTTCATGGTGTTCCTTGTAAGTTTCTTCTTTTTTGTCGTCATACGGGTGGTTCC
8: TCCGGTGGTAGGAGTGATAGTAGTCGTCCTGCGATTAAGGCTGGGTTTCCGGCTGGTGCTGTTGGTGGTTCC

Observed codon nucleotide distribution for library LC18, a targeted 54-mer library based upon analysis of the above eight sequences.

	X		Y		Z	
	Predicted	Actual	Predicted	Actual	Predicted	Actual
A	32	27	28	20	0	0
T	8	13	24	30	60	75
C	21	27	25	28	0	0
G	39	33	23	22	40	25

Representative sequences from library LC20, a targeted 54-mer oligonucleotide combinatorial library (underlined nucleotides correspond to the fixed Ser/Gly flanking sequences). For brevity, the flanking restriction site sequences (GGATCC and CTCGAG) are not shown. Surprisingly, three of the ten combinatorial site sequences examined from this library contained insertions or deletions. It is possible that these insertions or deletions are the result of sequencing errors, and are not actual changes in the size of the combinatorial oligonucleotide segment. However, at this point, it is not advantageous to resequence the clones, since it is sufficient to observe that the sequences show the expected randomness.

1: TCCGGTG TACTGTGCTTCATTCGTCTGCTCCTCGGCCTAATACTCCTCTTGAGCCTGAGTAGGGTGGTTCC
2: TCCGGTGGTACTCATGATGGTAGTAATGATCTTATTGGTTCTGTTCTTAATCAGAGGAGTGGTGGTGGTTCC
3: TCCGGTGGTTATTTTGGTCATAATCCTATTAATAACTATATTGCTACTTTTGATAATAGTACTGGTGGTTCC
4: TCCGGTGGTAGTAGCTTGAGGTTAATACTGTATCTTCTTCATCCTGCTCCTATTGTGAAT GGTGGTTCC
5: TCCGGTGGTCGGAGTGTTCCGACTAGTATTGCTCTTCCTGTTAGTCCTCCTTCCTCGTCTTGAGGGTGGTTCC
6: TCCGGTGGTAGTCCTCTTATTAATGATACGACGCCTCGGCTTAATGGTATTACTGGGACTCTTGGTGGTTCC
7: TCCGGTGGTATTCTTATTCATGTTAATACTTTTTTTACTACTAGTCGTCCTACTCATCTGTTGGGTGGTTCC
8: TCCGGTGGTAGGCTGACGACTGATACGGGTACTGCGACTGCTAATCCTAGTATTGGTGTGCATGGTGGTTCC
9: TCCGGTGGTTATAATCATCAGCAGGTTGTTTATAATCATTTTTTGCCTCTTATTGGTCATAATGGTGGTTCC
10: TCCAGTGGTCGTGTTACGCCTTATAGTGCTTATGTGGATACTGTTTCGTGTTCTAGTACTGATGGTGGTTCC

Observed codon nucleotide distribution for library LC20, a targeted 54-mer library based upon analysis of the above seven sequences that were of the expected size.

	X		Y		Z	
	Predicted	Actual	Predicted	Actual	Predicted	Actual
A	32	37	28	25	0	0
T	8	14	24	25	82	75
C	21	27	25	33	1	0
G	39	22	23	18	22	25

Titres of recombinant combinatorial retroviruses. Each combinatorial library cloned into our packaging plasmid ptatCCDlib-β-gal is produced in large quantities in bacterial cells and purified. Each packaging plasmid is combined with plasmids encoding *gag-pol* and the *VSV env,* and used to tranfect 293 cells with high efficiency. High titre, infectious, non-replicating, recombinant retroviruses are produced with this system, where each retrovirus contains RNA encoding one member of each combinatorial tat-CCD library and β–galactosidase. The β–galactosidase allows rapid determination of retrovirus titres and infection efficiency. Representative retrovirus titres for the combinatorial libraries are shown below:

Library	β-galactosidase titer (colony forming units/ml)
LC13	2.2×10^6
LC14	2.3×10^6
LC14r25	1.6×10^6
LC14r26	0.8×10^6
LC14r27	4.2×10^6
LC14r28	2.4×10^6
LC14r29	2.4×10^6

Infection efficiency of recombinant pantropic retroviruses. The recombinant retroviruses encoding our tat-CCD combinatorial protein libraries are termed pantropic, since they contain the VSV envelope protein as their major structural protein. The VSV envelope enables these retroviruses to infect all mammalian cells, with efficiencies approaching 100% as determined by β-galactosidase staining. Upon retrovirus infection, adaptein (i.e., tat-CCD combinatorial protein library) sequences are randomly integrated into the host cell genome. Since these sequences are flanked 5' by a strong promoter, the adaptein protein is expressed to high levels, and targeted to the cytosol. Immunofluorescence (IF) experiments, using polyclonal antibodies to the CCD protein, confirm that adaptein expression is observed in the cytosol of ~100% of infected cells.

Improved and novel technology:

Methods such as phage display have been successful because small populations of ligand-presenting phage can be amplified out of a larger library of phage. Similarly, we have devised a method to rapidly amplify library components with a desired phenotype/function from the retroviral library (Figure 2).

Briefly, cells are infected with the vector and then selected with the cytopathic agent. Over the next 3 days resistant cells will survive and form colonies. However, our observations indicate that some cells escape the selective agent. This may be due to mutation, growth status of the cells, culture conditions etc. Because we routinely infect at a multiplicity of infection of >1 then both populations carry library components. To **enrich for the functional component** we have optimized conditions to regenerate a subpopulation of retroviruses. These are introduced into new cells and then the

process is repeated. After 3-4 rounds we should have enriched for the functional population.

Continuing the process should select for the most potent library components. As a test we infected cells with a β-galactosidase encoding retrovirus at an MOI of 0.01. We then regenerated the retrovirus. Given a transfection efficiency of 50% (typically this is 80%) and the fact that 5×10^6 cells yield approximately 10^7 infectious virions, this indicates that we can expect to recover virus from all cells surviving selection (colonies typically 8 cells after 3 days).We are currently testing this system and expect to have results by the next progress report.

Construction of an alternative EGFP based scaffold for library presentation.

We have produced a second library based on an EGFP scaffold. This permits us to track expression of the library and titer of library encoding virus stocks directly. As of 10/21/02 the library was introduced into cells at an MOI of 5. Expression is comparable to EGFP alone and high with complete coverage of the target cells (Figure 3).

Rickettsial challenges

The initial rickettsial challenges were performed using murine splenic endothelial cells (SVEC). We have had extensive experience with this cell line in the laboratory in regards to rickettsial infection. A total of eight Petri dishes were infected with retroviruses encoding adaptein libraries. Adequate negative controls were included in the experiment (retroviruses containing no adaptein libraries). Productive retroviral infection of the monolayers was monitored by β-galactosidase staining. Between 90-100% of the cells were documented to be infected. After 48 hours of inoculation with the retroviruses, the cell monolayers were challenged with 1 MOI of yolk-sac derived *R. rickettsii*. The flasks were observed on a daily basis for 8 weeks. The monolayers were trypsinized at 4 weeks and seeded in T-25 flasks. No differences were noted between the different Petri dishes infected with adaptein-encoding retroviruses and non-adaptein encoding retroviruses. A second experiment using the same protocol was performed producing the same results. At the end of eight weeks two T-25 flasks were lost because of bacterial contamination, and the cell monolayers detached from the remaining six flasks. Even though these experiments did not yield any positive results (detection of protected cells against rickettsial challenge), several useful observations were made during these two experiments. First of all, the cellular death rate for SVEC cells with 1 MOI was not high enough to allow for fast screening and detection of adaptein-protected cells. The proliferation rate of SVEC is high even under low-serum conditions. Secondly, heavily infected monolayers detached as large clumps of cells instead of single cells detaching individually. Thirdly, the infection of the monolayer was noted to be patchy and not regularly distributed, a finding that we attributed to the presence of yolk sac material in the inoculum that tends to cause clumping of rickettsial organisms. The next set of experiments involved the study of cell death dynamics in infected monolayers. Because of the phenotypic observations made with SVEC cells, we decided to use Vero cells for the next round of experiments. Furthermore, we decided to use renografin-purified organisms to enhance even distribution of the infection across the Vero cell monolayers. The first experiment with Vero cells consisted of infecting several T-25 flasks with 10 MOI of *R. rickettsii*. The cells were then fixed, permeabilized and stained with propidium iodide 48 hours after inoculation to evaluate homogeneity of infection across the monolayer. By using renografin-purified rickettsiae, we noticed that the distribution of infected cells was far more homogenous when compared to yolk-sac derived rickettsiae. In the second experiment, we quantified the amount of cell death after inoculating Vero cells in T-25 flasks with 1 MOI of *R. rickettsii*. Cell death was detected by exclusion of propidium iodide from live cells and nuclear staining in dead cells. The cell monolayers were evaluated daily for 96 hours. An average of 30-40 dead cells were observed in each high power field (HPF) evaluated. By comparison, 3-5 dead cells per HPF were observed in non-infected monolayers. By the end of 96 hours, more than 50% of the cells were still present in the monolayers. We then decided to increase the MOI to 10 in order to enhance cellular killing. We also decided to use sulfoximine in order to decrease intracellular glutathione levels and enhance cellular

killing. We treated cell monolayers for 24 hours with sulfoximine previous to rickettsial inoculation. Sulfoximine-treated and non-treated cell monolayers were then infected with 10 MOI of *R. rickettsii* (Figure 4, Table 1). We are in the process of conducting more experiments increasing the MOI to 50 and treating the cell monolayers continuously with sulfoximine. We are also optimizing cell killing for *R. prowazekii* and *O. tsutsugamushi*. The rationale behind all these preliminary experiments is to optimize cellular killing by rickettsiae so that we can screen for adaptein-protection as efficiently as possible. We have plans to start a new round of rickettsial challenges in the middle of March. Vero cells will be infected with adaptein- and non-adaptein-containing retroviruses at 20% confluency and 1 MOI. After 48 hours of retroviral inoculation, the monolayers will be infected with *R. rickettsii* and examined daily with phase contrast microscopy. After 96-120 hours, the monolayers will be trypsinized and plated. This step will select cells resistant to the challenge. Infected cells will not be able to reattach to the flasks. Five to six rounds of trypsinization and plating will be conducted with the purpose of enriching the population of resistant cells. At that point, the remaining cells will be rechallenged with rickettsiae, and cell viability will be determined.

B. Specific aim #2: To determine the roles of NF-κB, ctyokines (TNF-α, IFN-γ, RANTES), ROS and NO in intracellular killing of rickettsia-resistant monolayers.

We have just started experiments related to specific aim #2. At this time we are conducting experiments to determine the effect of ROS in intracellular killing of cell monolayers infected with rickettsiae.

C. Specific aim #3: To characterize signal transduction pathways modulating the cytoskeletal events responsible for the increased vascular permeability seen in rickettsial infections.

An endothelial cell line (RBE4) derived from rat brain microvascular endothelial cells was obtained from Dr. Francoise Roux in France. The cells were first characterized by using acetylated LDH uptake confirming their endothelial derivation. Subsequently, the cells were tested by PCR for mycoplasma infection before propagating them in the laboratory. After the characterization stage, the cells were propagated in collagen-coated transwells with 0.4 μm pores (Corning Costar Co.) until they formed monolayers. The optimal seeding density was obtained empirically by culturing the RBE4 cells at different concentrations. A concentration of 400,000 cells/ul was found to be ideal so that monolayers were formed in 24-48 hours.

Studies of endothelial permeability

For the initial experiments of vascular permeability, FITC-dextrans of four different molecular weights were used (4,400, 9,800, 38,200 and 77,000 Da). The first step was the validation of this technique with the Perkin Elmer fluorimeter. Ten consecutive two fold dilutions of 0.3 nM of each FITC-dextran were diluted in PBS with magnesium and calcium. The relationship between fluorescent intensity and concentration of the fluorescent dextrans was determined to be an hyperbolic function, especially with the high molecular weight dextrans. The experiment was then repeated by adding 10% formaldehyde to the FITC-dextran suspensions in order to check for possible alterations in fluorescent emission. The purpose of this experiment was to validate the technique in the presence of formaldehyde due to the fact that formaldehyde was going to be used at the time of the experiments involving *Rickettsia*-induced changes in vascular permeability. No differences were noted between fixed and non-fixed FITC-dextran suspensions.

Cell monolayers grown in transwells were then used for baseline experiments with FITC-dextrans in order to detect baseline permeability values for each of the different molecular weight dextrans. The FITC-dextrans were added to the "luminal" or upper chamber of the transwells and serial samples were obtained from the "abluminal" or lower chamber of the transwells at 0, 15, 30, 60, 90, 120, 150 and 180 minutes. Minimal "leakage" of dextrans was seen at all time points. In addition, the baseline permeability was greater for lower molecular weight dextrans as expected. Once these baseline

experiments were finalized, cell monolayers were infected with 50 MOI of egg-yolk sac-derived *Rickettsia rickettsii,* and the abluminal chamber was sampled serially at 0, 60, 90, 120, 150, and 180 minutes, 6 hours and 24 hours. Initial results suggest that alterations in vascular permebaility are present after a high inoculum of rickettsiae is added to RBE4 cells (Figure). The differences become more apparent between infected and non-infected monolayers after 90 minutes of infection for the lower molecular weight dextrans and after 120 minutes for the high molecular weight dextrans. Experiments with renografin purified rickettsiae are currently underway to confirm these results obtained with yolk-sac grown rickettsiae.

Electric Cell-Substrate Impedance Sensing (ECIS) Analysis

By applying current and measuring the voltage across a small empty electrode, the impedance can be calculated and broken down into a series resistance and capacitance. When cells attach and spread upon the electrode, they do not respond in any way to the very weak AC current, but their insulating membranes block and constrain the current flow, resulting in measured variations in the impedance. From these impedance changes, several properties of the cell layer can be determined such as morphology changes, barrier function, cell motility, cell surface coverage, membrane capacitance and the average spaces beneath the cells (11-12). A typical ECIS-generated Resistance vs. Time graph (using NRK cells) is illustrated below in Figure 5.

Our laboratory acquired ECIS technology for use in the BSL-3 laboratories last year. The initial experiments with this new technology are highly encouraging. With this new technique we will be able to replace transendothelial electrical resistance measurements (TEER), as planned initially. TEER is cumbersome and requires intact monolayers across a large surface for correct measurements. With ECIS, measurements of electrical resistance across monolayers can be performed with as few as 100-200 viable cells across the electrode.

In our experiment using RBE4 cells, the chart labeled "RBE4 Seeding/Spreading" clearly shows that seeding with 10^4 cells were insufficient for the monolayer to become confluent within 40 hours of the assay period. Instead, we can see that approximately 80 hours were required to complete spreading (1.0E+04 RBE4 Cells Control. Figure 6). *R. rickettsii* were inoculated at time = 0 hour (i.e., approximately 40 hours after seeding), and the responses of the RBE4 cells were monitored for a total of 80 hours post-inoculation (Figures 7-8). Thus, the chart labeled "*R. rickettsii* Inoculation (Continue)" represents the response curves 40 – 80 hours after inoculation, or 80 – 120 hours after seeding. Regardless of the seeding density, the permeability of the RBE4 cell monolayers was greatly compromised by the rickettsial infection as evidenced by the dramatic drop in resistance across the monolayer. This effect was dose dependent. Figure 8 clearly shows the dramatic decrease in resistance and the lack of fluctuations (due to cell motility) of the response curves at approximately 55 and 60 hours post-inoculation (1.0E+05 RBE4 Cells + 1.5E+08 pfu and 1.0E+05 RBE4 Cells + 1.5E+07 pfu, respectively). The decrease in resistance and micromotility observed in the control (1.0E+05 RBE4 Cells Control) is attributed to the normal cell death and subsequent detachment due to nutrient exhaustion as media were not changed during the course of the experiment. The 10^4 RBE4 cells control (1.0E+04 RBE4 Cells Control) showed virtually no change in response, most likely due to the 10-fold less seeding amount, and therefore nutrients in the media were not exhausted, and metabolic by-products had not accumulated significantly to harm these cells.These results confirm the data obtained with the FITC-dextrans, although changes in permeability were observed earlier in such experiments. However, rickettsial inocula were not standardized for both experiments. We are planning to standardize all conditions and perform the experiments in parallel in order to resolve the discrepancies.

At this point we have not performed experiments to elucidate if this phenomenon was due to compromised intercellular junctions, increased transcellular flow or massive cell death. Experiments

to answer those questions are underway. To evaluate intercellular junctions, we will measure inulin concentrations in transwells. For evaluation of transcellular flux, fluorescent tracers will be used to semiquantitate cytoplasmic fluorescence. For cell death in the monolayers, we will evaluate the integrity of the monolayers with propidium iodide in parallel with ECIS monitoring.

We will also be performing the same experiments with *R. prowazekii* and *O. tsutsugamushi*. In addition, the role of cytokines and products of the coagulation cascade in endothelial permeability will be studied. By using a unique feature in the ECIS system, we will also be able to determine the role of paracellular and transcellular permeability separately. The information obtained with the latter experiments will be important in determining the role of junctional proteins and pinocytotic processes as they relate to endothelial permeability.

Immunohistochemical studies performed with RBE4 cells have failed to demonstrate expression of occludin and ZO-1, two tight junction proteins expressed in epithelia and endothelia in the body. Stains with adherens junction proteins (cadherins, α-, β-, and γ-catenins) did not reveal dramatic changes during rickettsial infections by fluorescent microscopy. Experiments using primary endothelial cells derived from rat or mouse brain are being planned in order to study the role of tight junction proteins. In addition, RBE4 cells will be co-cultured with rat glioma cells (C6) in order to induce expression of tight junction proteins.

Intracellular calcium measurements after rickettsial internalization

For measurements of intracellular calcium, RBE4 cells were loaded with Fluo-3, a molecule that emits fluorescence in the green spectrum. The intensity of the fluorescence depends on the calcium levels present in the intracellular environment. Optimization of cell loading was performed at different temperatures, incubation times and probe concentrations. The ideal conditions for loading were 30 minutes of incubation time with 1.25 μmol of Fluo-3 at 25 °C. Fluo-3 responses to calcium levels were tested with ionomycin.

Rickettsia-infected RBE4 monolayers were then infected with *R. rickettsii,* and changes in fluorescence were monitored up to 24 hours. Increased fluorescent levels were detected at 1 hour and up to 24 hours (Figure 9). Quantitative measurements by using calibration curves will be performed as soon as specialized software and confocal microscopy are made available in the BSL-3 environment. However, these initial results confirm elevation of intracellular calcium levels after infection with pathogenic rickettsiae in endothelial cells.

Determination of calmodulin activation

24-well plates were seeded with SVEC cells (lymph modal capillary high endothelial cells) at a concentration of 100,000 cells /ml and grown to 50-60% confluency at 37 °C overnight in DMEM with 10% fetal bovine serum.

TOP10 *E. coli* was transformed with plasmids pCDIC-38 and YC2.3 containing the coding sequences of CFP and YFP linked by smooth muscle MLCK calmodulin binding domain in the first plasmid and M13 and the calmodulin calcium binding domain in the second plasmid. The plasmids were then purified with QIAGEN Plasmid Midi purification kit

Characterization of the plasmid was then carried by using restriction enzymes XhI and *Hind* III. The sequence of the linkers was confirmed by amplifying these fragments of the vector by PCR with the forward primer EYFP-F (5'-GTT GTG GGT GTT GCA GAT ATA GTA -3') and reverse primer

ECFP-R (5'- TCA CCG CCG ACA AGC AGA AGA AC -3'). The cycles comprised an initial incubation at 94 °C for 120 sec. followed by 35 cycles (94 °C for 30 sec; 55 °C for 30 sec and 72 °C for 30 sec) and a final extension at 72 °C for 7 min.

The PCR product was then purified with the QIA quick PCR purification kit and sequenced by the dideoxynucleotide method of cycle sequencing with *Taq* polymerase. The sequencing reaction was carried out for each strand of DNA to avoid possible errors of incorporation of nucleotides.

The cell monolayers were then transfected at semiconfluency with both plasmids by using LipofectAMINE PLUS reagent. Optimization of the transfection protocol was performed according to manufacturer's instructions by using different concentrations of plasmid DNA (range:1.0-1.6μg). Transfection efficiency was evaluated 24-48 hours later by fluorescent microscopy with an inverted NIKON microscope equipped with a CFP/YFP excitation/ emission filter.The transfected monolayers were then infected with *Rickettsia montanensis* and changes in fluorescence emission were monitored for up to 24 hours. Internalization of *R. montanensis* by SVEC cells was demonstrated by Diff Quik stain.

Transfection efficiency was between 60-70% of cells at plasmid concentrations between 1.3 and 1.6 μg. The transiently transfected cells infected with *R. montanensis* were then monitored under fluorescent microscopy. Up to 24 hours post infection, loss of FRET was detected in the cell monolayers infected with *R. montanensis*, and transfected with plasmid pCDIC-38 as evidenced by an increase in the cyan emission from the cells upon excitation at 433 nm . Increased FRET was observed in cells transfected with plasmid YC2.3. Positive (ionomycin added to medium) and negative controls (non-transfected cells, and transfected non-infected cells) were used (Figure 10). We will be performing these experiments during the second year with RBE4 cells and *R. rickettsii, R. prowazekii and O. tsutsugamushi*.

Myosin light chain experiments

Approximately 4.5 x 10^9 pfu of *R. rickettsii* were used to inoculate T-150 flasks of confluent RBE4 cells. Absorption was carried out for one hour at 37°C. At the end of the absorption period, *R. rickettsii* that had not been absorbed were removed by suction, and 25 ml of RBE4 growth medium supplemented with 1% fetal calf serum was added. Incubation was carried out at 37°C without CO_2 for one or three hours. Cell lysis was carried out using M-PER® mammalian protein extraction reagent (Pierce) per manufacturer's protocol. Rabbit polyclonal antibody (purified IgG) raised against full length myosin regulatory light chain (MLC) used in the western blot experiment was purchased from Santa Cruz Biotechnology, Inc. The top band represents the non-phosphorylated MLC and the bottom band represents the mono-phosphorylated form of MLC. A decrease in myosin phosphorylation was observed at 3 hours (Figure 11). The significance of this observation is unknown. Experiments are currently underway to extend the time points to better evaluate the role of myosin phosphorylation in endothelial permeability.

III. KEY RESEARCH ACCOMPLISHMENTS

Construction of two dozen libraries using plasmid ptatCCDlib-β-gal encoding combinatorial 6-mer, 12-mer and 18-mer peptides.

Succesful large scale production of combinatorial libraries in bacterial cells.

Succesful transfection of two different cell lines (SVEC and Vero cells) with recombinant retroviruses containg libraries with high efficiency. These cell lines are being used for rickettsial challenges.

Development of in vitro models of endothelial barrier using rat-derived brain microvascular endothelial cells.

Measurements of endothelial permeability by using ECIS and FITC-dextrans.

Succesful transfection of endothelial cells with CFP-YFP containing plasmid for detection of calmodulin activation by FRET.

IV. REPORTABLE OUTCOMES

Abstracts and presentations

1. Houston Society of Clinical Pathology. Pathology of Selected and Potential Bioterrorist Agents. 2002.

2. **Olano JP**, Wen G. Evidence of calmodulin activation in an *in vitro* model of rickettsial infection. American Society of Investigative Pathology. FASEB J. 2002;16:A202.

3. **Olano JP** and Wen G. Evidence of calmodulin activation in rickettsial infections. Poster and Podium presentation. American Society of Investigative Pathology. New Orleans, 2002.

V. CONCLUSIONS

In summary, several goals have been accomplished during the first year of funding of this project. During the initial months of the grant, training of the key personnel to work in the BSL-3 environment took place. In addition, large stocks of the infectious agents to be used in the experiments were produced.

We successfully developed approximately two dozen different combinatorial protein libraries with diversities of ~10^7-10^8. These libraries are encoded within, and delivered by, either recombinant retroviruses or episomal plasmids. The libraries encode 6-mer, 12-mer and 18-mer peptides. Large scale production of the combinatorial libraries was achieved in bacterial cells and subsequently purified. We then were able to transfect two cell lines that are being used for rickettsial challenges. In the coming year we will attempt to improve our cloning protocol to achieve more diversity in our libraries (~10^9 members). In addition, we will also try to transfect a macrophage cell line and an additional endothelial cell line (RBE4) for rickettsial challenges.

We also have achieved progress in other specific aims of the project. We have demonstrated elevation of intracellular calcium levels in SVEC cells infected with rickettsiae. Quantitative experiments are underway. Even though quantitative measurements of intracellular calcium have not been performed, we think that such levels are high enough to induce calmodulin activation as demonstrated in vitro in SVEC cells by FRET. The significance of calmodulin activation is at this point unknown, but it is possibly related to phosphorylation of MLCK with subsequent phosphorylation of myosin. Preliminary experiments by Western blotting showed decreased levels of phosphorylated myosin early after rickettsial infection. We are currently extending the time points in this experiment to fully evaluate the significance of myosin phosphorylation. Experiments desgined to study endothelial permeability by ECIS and its relationship to calcium signaling and myosin phosphorylation are currently being planned.

VI. SCIENTIFIC PERSONNEL

a. David H. Walker M.D. Principal Investigator (10% effort)
b. Juan P. Olano M.D. Co-Investigator (25% effort)
c. Stanley J.Watowich Ph.D. Collaborator (10% effort)
d. Robert A. Davey Ph.D. Collaborator (10% effort)
e. Paul Koo Ph.D, Post-Doctoral fellow.
f. Olga Kolokoltsova. Research Technician
g. Drew Deniger. Research Technician

VII. REFERENCES

1. Raoult D, Roux V. Rickettsioses as paradigms of new or emerging infectious diseases. Clin Microbiol Rev 1997;10(4):694-719.
2. Walker DH, Zavala-Velazquez J, Ramirez G, Olano J. Emerging infectious diseases in the Americas. In: Raoult D, Brouqui P, editors. Rickettsiae and rickettsial diseases at the turn of the millenium. Paris: Elsevier; 1999. p. 274-277.
3. Walker DH. Rocky Mountain spotted fever and other rickettsioses. In: Schaecter M, Engleberg NC, Eisenstein BI, Medoff G, editors. Mechanisms of microbial disease. Baltimore: Williams & Wilkins; 1998. p. 268-274.
4. Walker DH, Dumler JS. Rickettsial infections. In: Connor DH, Chandler FW, Schwartz D, Manz HJ, Lack EE, editors. Pathology of infectious diseases. Stamford: Appleton & Lange, Inc.; 1997. p. 789-799.
5. Atlas RM. Biological weapons pose challenge for microbiology community. ASM News 1998;64:383-389.
6. Moran GJ. Threats in bioterrorism. II: CDC category B and C agents. Emerg Med Clin North Am 2002;20(2):311-30.
7. Greenfield RA, Drevets DA, Machado LJ, Voskuhl GW, Cornea P, Bronze MS. Bacterial pathogens as biological weapons and agents of bioterrorism. Am J Med Sci 2002;323(6):299-315.
8. Henderson DA. The looming threat of bioterrorism. Science 1999;283(5406):1279-82.
9. Walker DH, Popov VL, Wen J, Feng HM. *Rickettsia conorii* infection of C3H/HeN mice. A model of endothelial-target rickettsiosis. Lab Invest 1994;70(3):358-68.
10. Dignat-George F, Teysseire N, Mutin M, Bardin N, Lesaule G, Raoult D, et al. *Rickettsia conorii* infection enhances vascular cell adhesion molecule-1- and intercellular adhesion molecule-1-dependent mononuclear cell adherence to endothelial cells. J Infect Dis 1997;175(5):1142-52.
11. Sandoval R. et.al. Ca (2+) signaling and PKC-alpha activate increased endothelial permeability by disassembly of VE-cadherin junctions. J Physiol 2001;533:433-445.
12. Tiruppathi C. et.al. Electrical method for detection of endothelial cell shape change in real time: assessment of endothelial barrier function. Proc Natl Acad Sci. 1992;89:7919-7923.

VIII. APPENDICES (TABLES, FIGURES, ABSTRACTS)

Table 1.

Effect of DL-buthionine-[S,R]-sulfoximine on *Rickettsia rickettsii*-induced cytotoxicity in Vero cells.

Time points	Groups	Dead cells/HPF (Mean ± S.D.)
24 hours	Control	2.1 ± 0.99*
	Infected	8.0 ± 2.26*
	Infected + sulfoximine	14.0 ± 4.08*
48 hours	Control	3.7 ± 1.33*
	Infected	14.2 ± 3.58*
	Infected + sulfoximine	22.4 ± 5.4*
72 hours	Control	3.7 ± 1.49*
	Infected	32.7 ± 8.30
	Infected + sulfoximine	42.2 ± 12.79
96 hours	Control	5.0 ± 1.5
	Infected	Monolayers lifted up
	Infected + sulfoximine	Monolayers lifted up

* Differences between all groups were statistically significant at $p < 0.001$ by the t-test except for the difference between the monolayer infected with *R. rickettsii* alone and infected with *R. rickettsii* and sulfoximine at 72 hours.

Figure 1

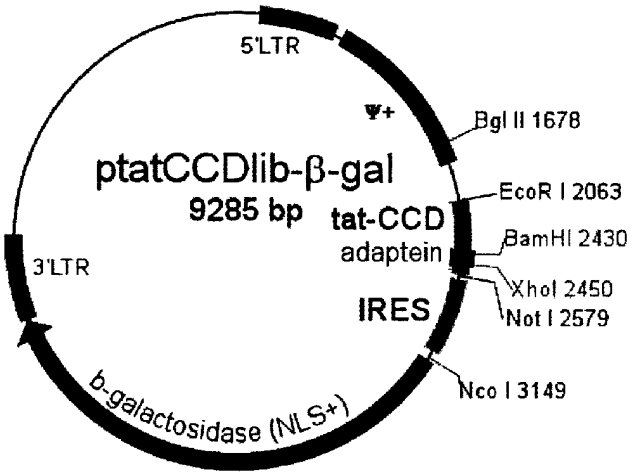

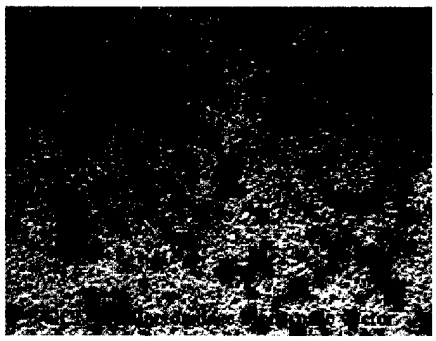

Left: Map of retrovirus packing plasmid, encoding a combinatorial protein library and β-galactosidase. The combinatorial cDNA is cloned into the *BamHi*/*Xho*1 sites, and expression of the resulting tat-CCD-library protein driven by LTR promoter. β-galactosidase expression is driven independently by the IRES.
Right: Use of bicistronic vector encoding the CCD peptide library and β-galactosidase marker for direct determination of titer. MOI of 0.1 used.

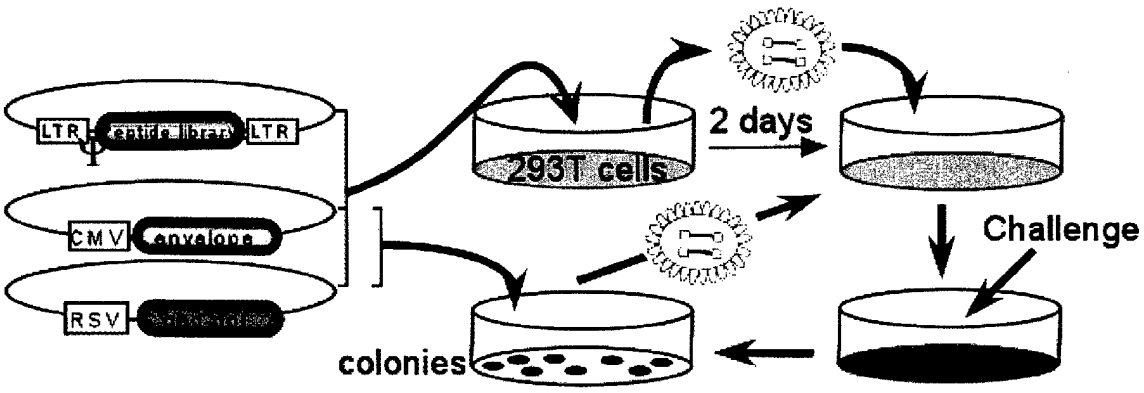

Figure 2

Retroviral repackaging method to amplify active library components from mixture. Generation of library involves introduction of 3 plasmids encoding peptide library, virus envelope protein and structural proteins (gag-pol). After introduction into cells and challenge with cytopathic agent, colonies form. Some resist the agent due to library expression; others survive because of random mutations, growth state of the cell, etc. Transfection of these cells with just virus structural and envelope proteins repackages the library components for rechallenge. Cycles amplify the protective library components and eliminate the random non-specific components.

Figure 3

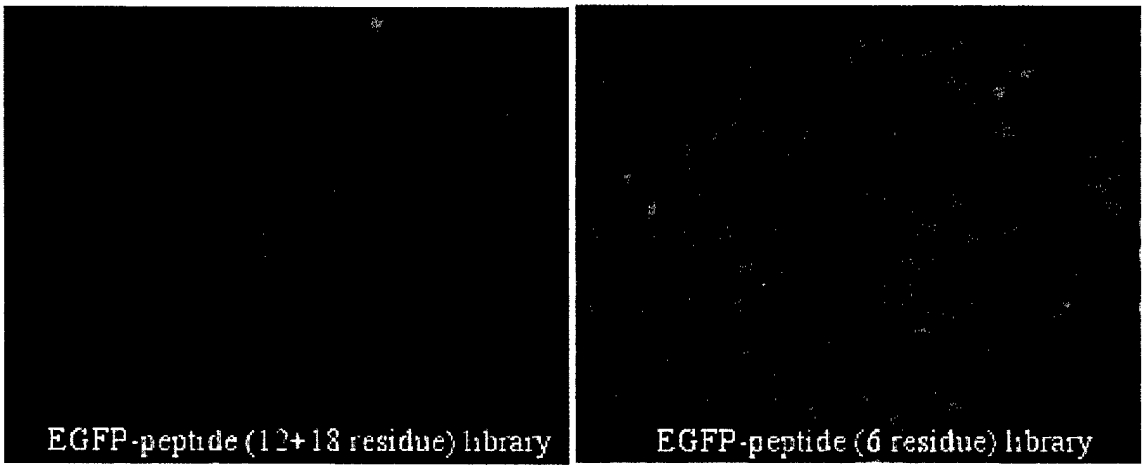

EGFP expression in cells infected (MOI of 5) with 12 and 18 residue (pooled) (left) and 6 residue (right).

Figure 4 . Kinetics of Cell Death after *R. rickettsii* Infection of Vero Cell Monolayers (MOI ~ 10, Magnification = 400X)

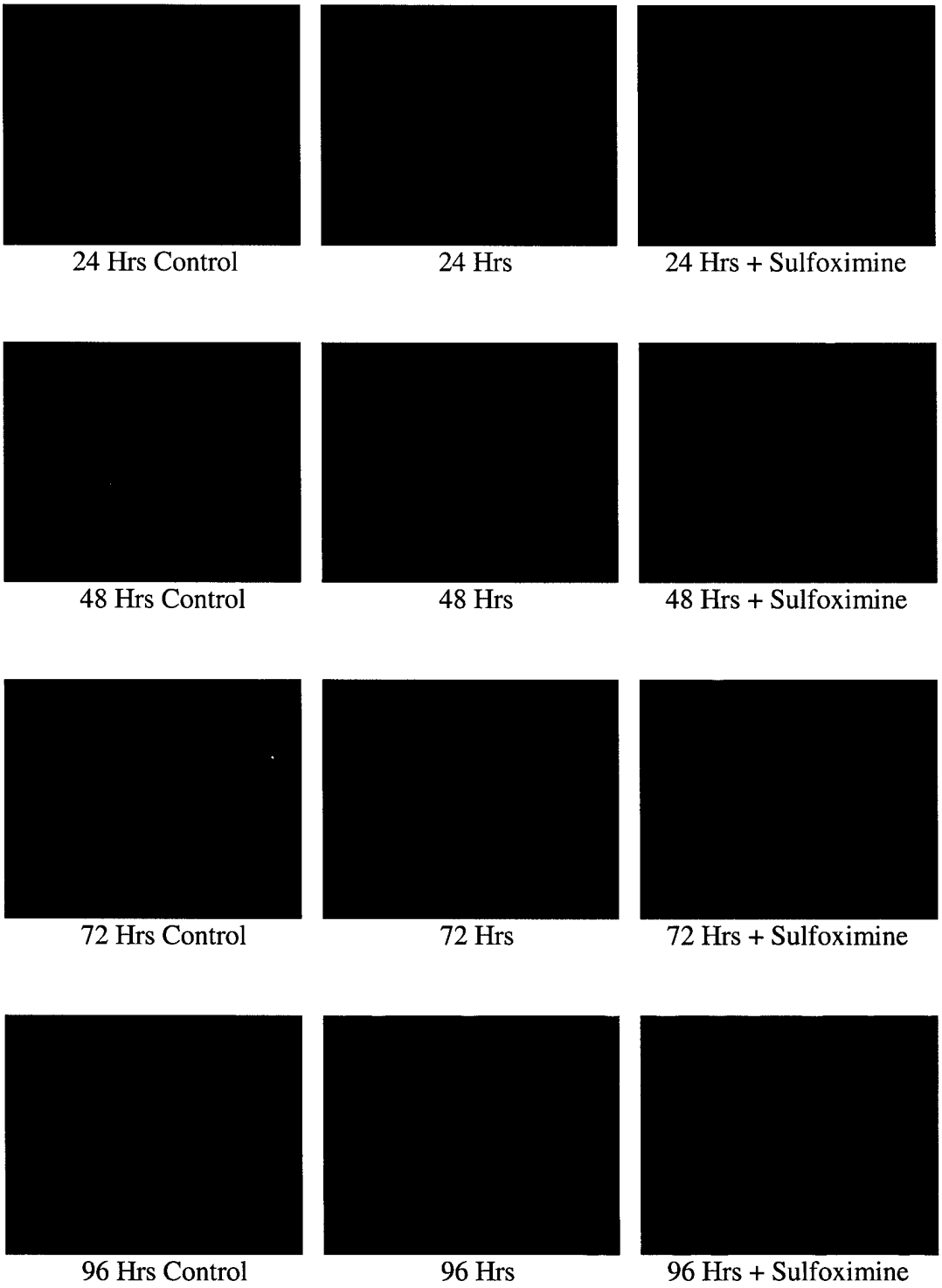

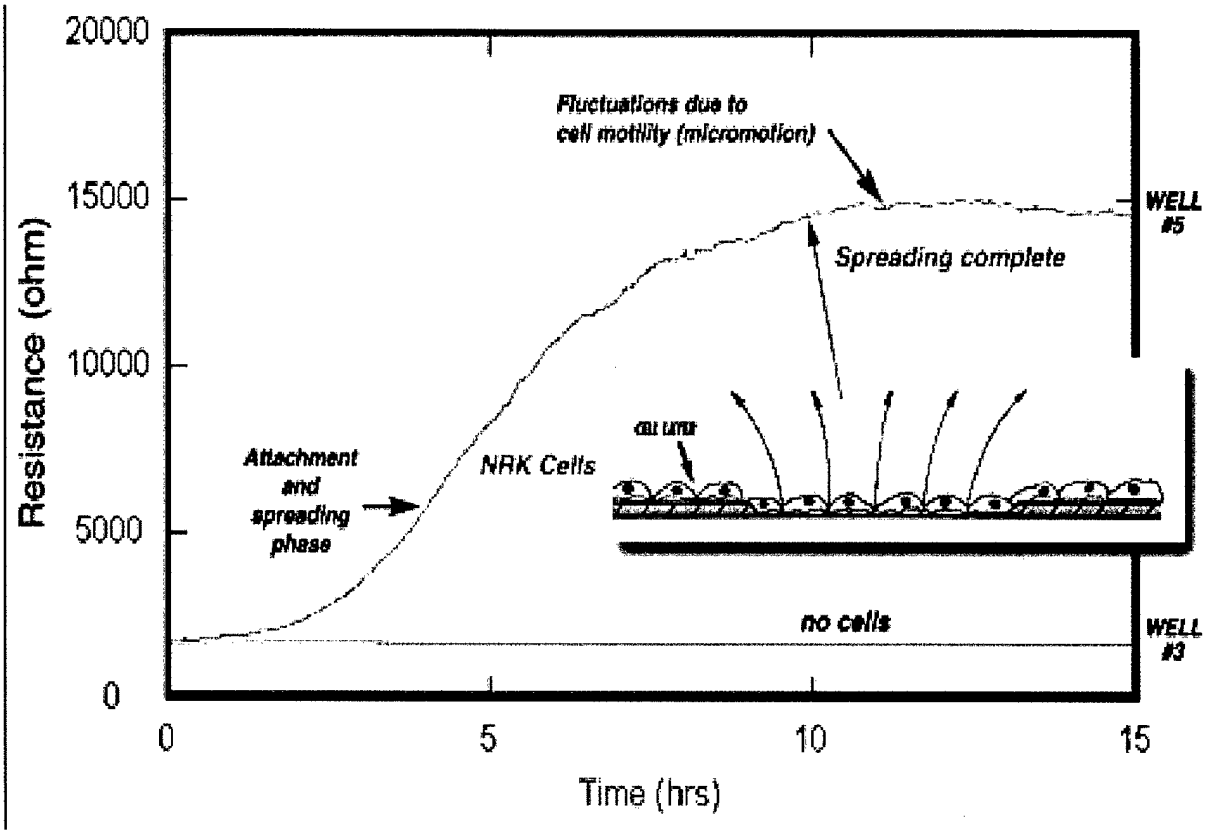
20000
15000
10000
5000
0
Resistance (ohm)
0
5
10
15
Time (hrs)
Fluctuations due to
cell motility (micromotion)
Spreading complete
WELL
#5
Attachment
and
spreading
phase
NRK Cells
cell unit
no cells
WELL
#3

Figure 5

Figure 6
RBE4 Seeding/Spreading

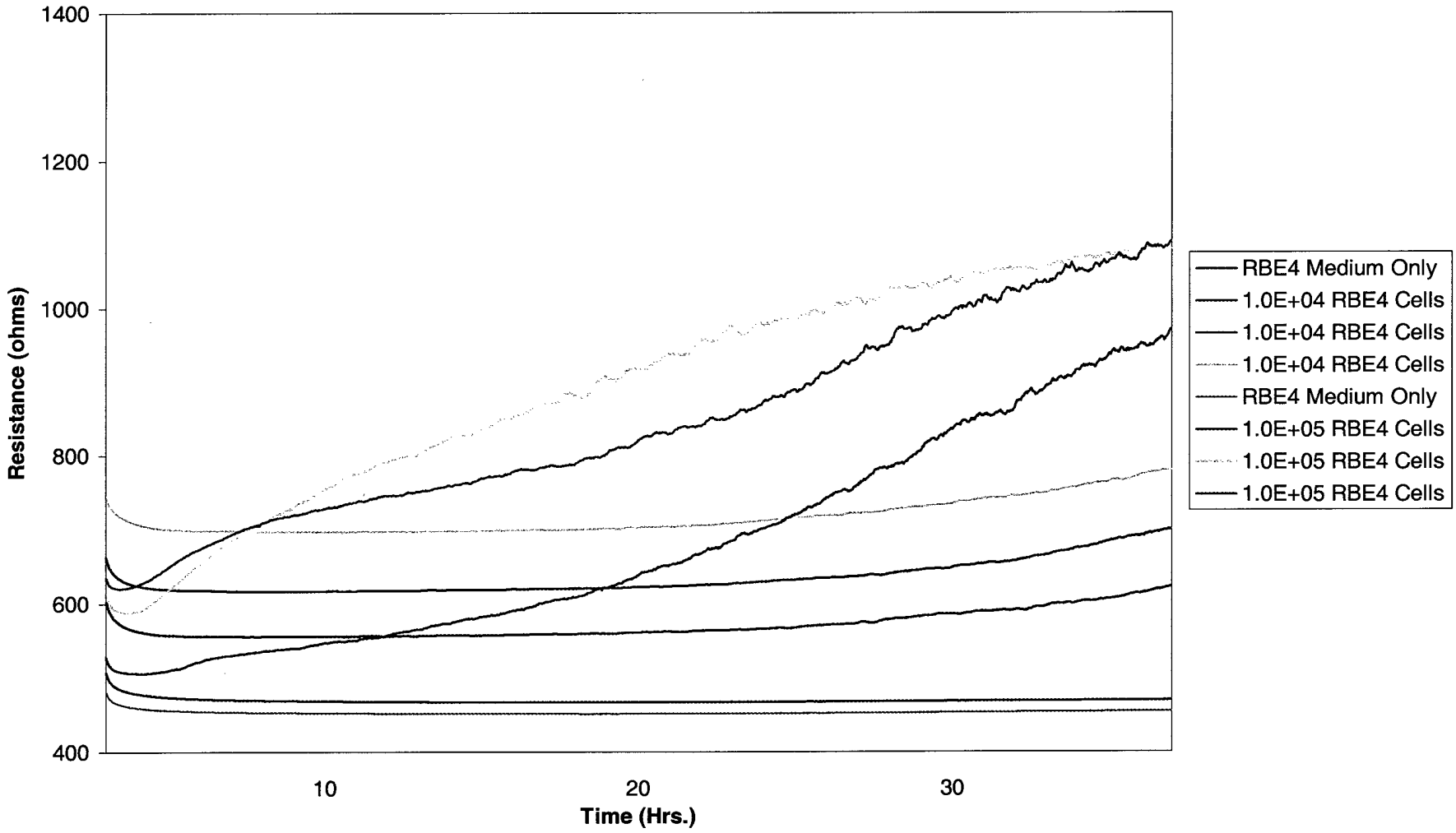

Figure 7
***R. rickettsii* Inoculation**

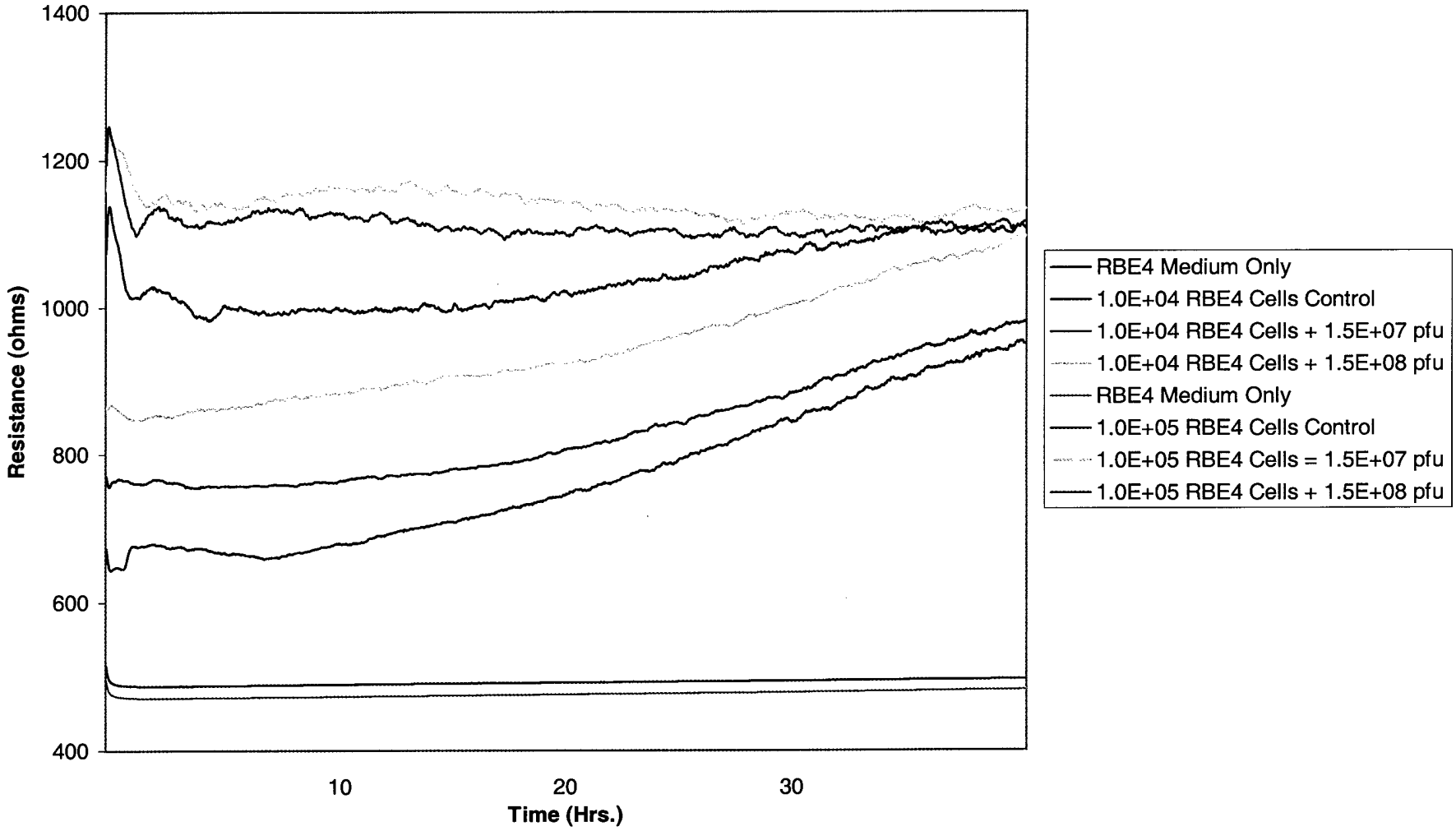

Figure 8
***R. rickettsii* Inoculation (Continue)**

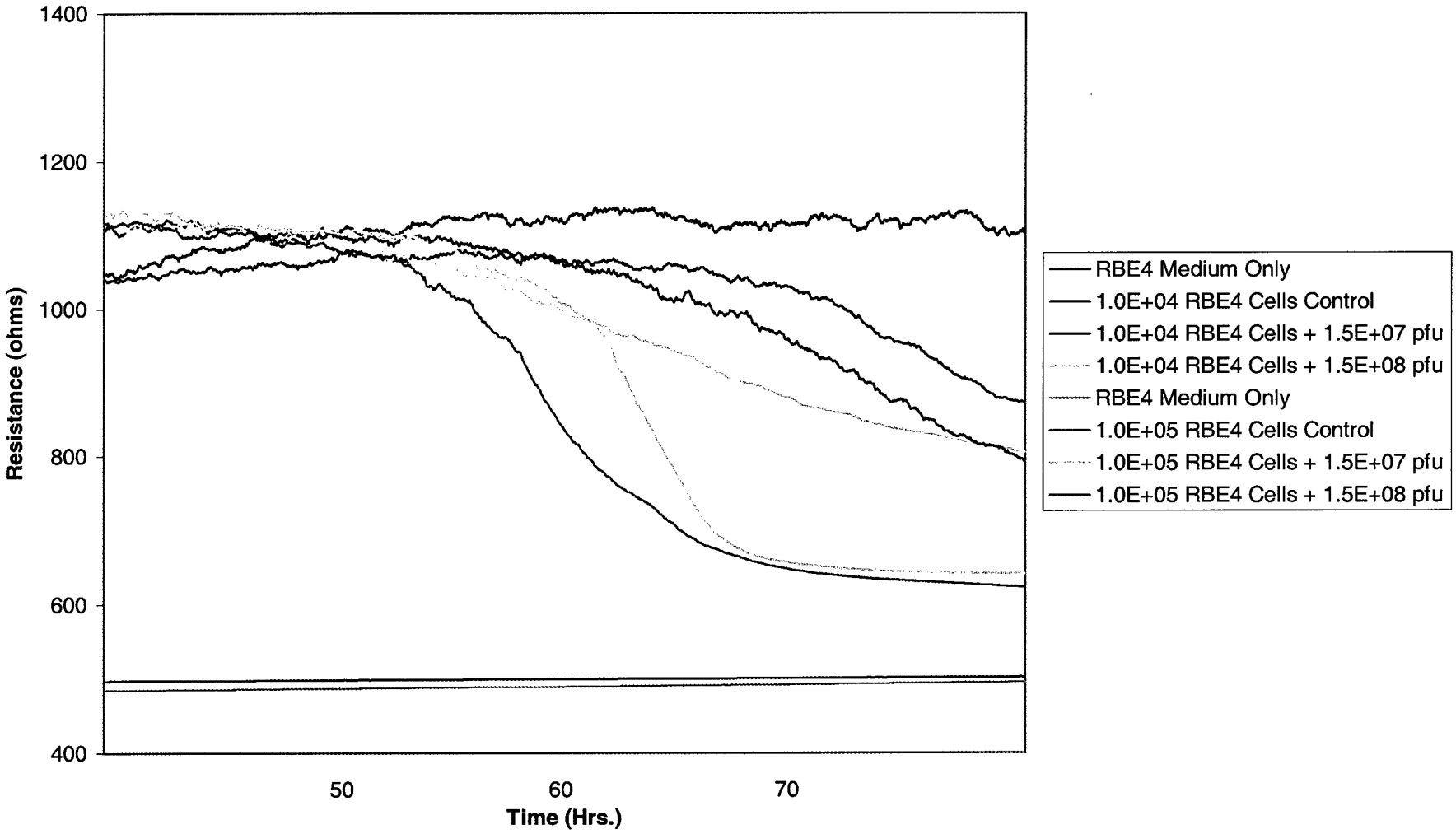

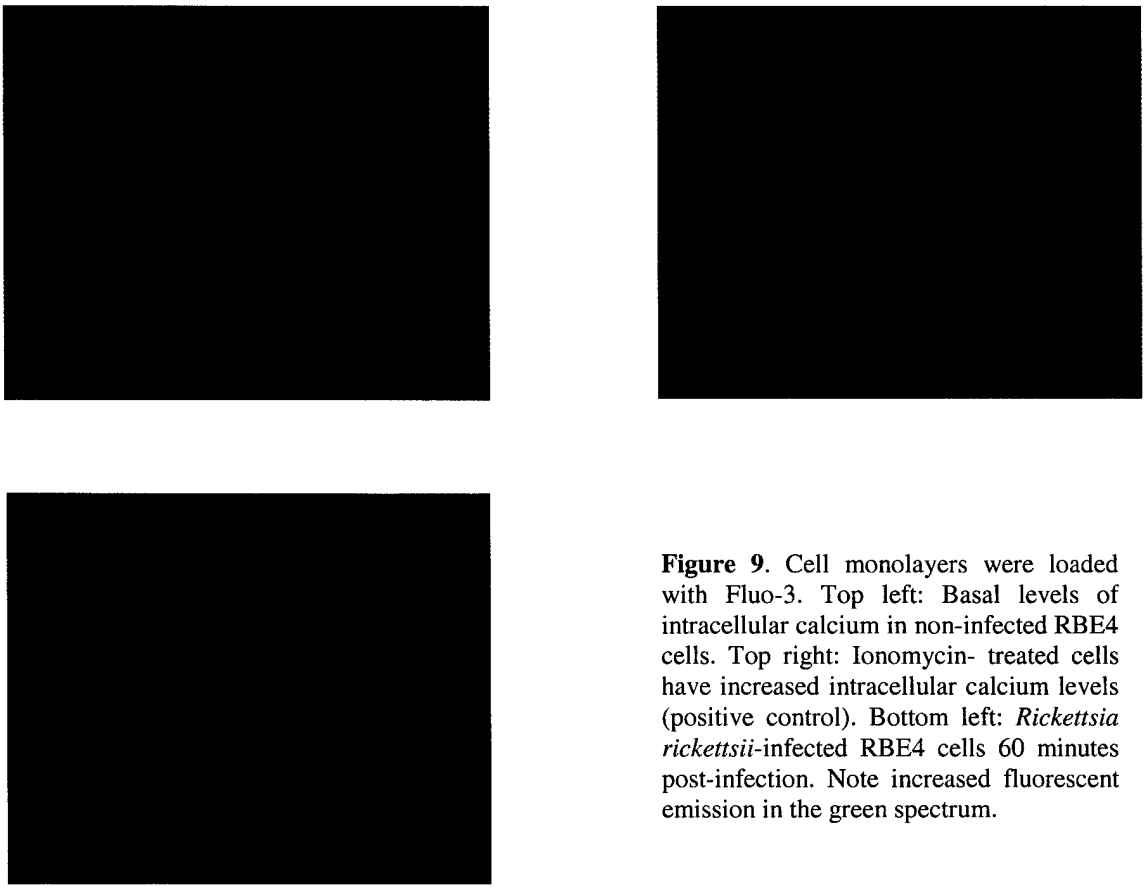

Figure 9. Cell monolayers were loaded with Fluo-3. Top left: Basal levels of intracellular calcium in non-infected RBE4 cells. Top right: Ionomycin- treated cells have increased intracellular calcium levels (positive control). Bottom left: *Rickettsia rickettsii*-infected RBE4 cells 60 minutes post-infection. Note increased fluorescent emission in the green spectrum.

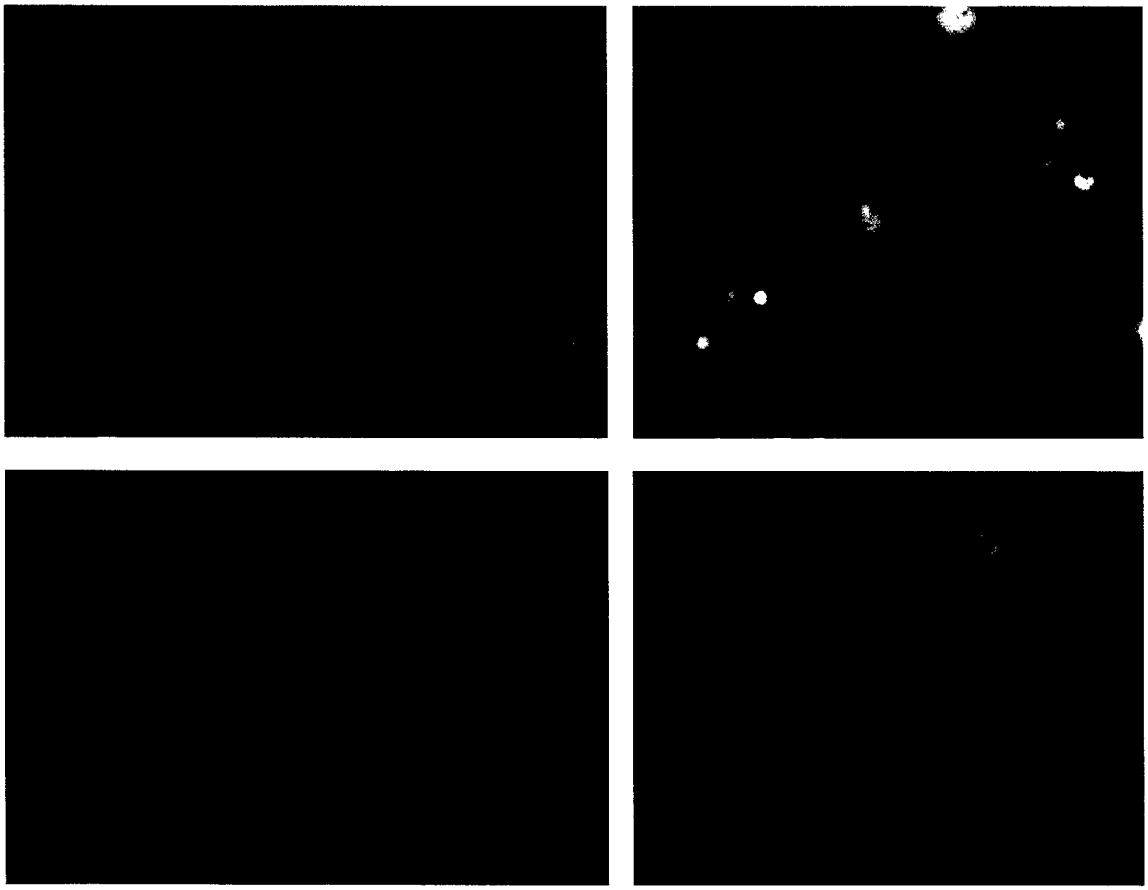

Figure 10.

Transfection efficiency was between 60-70% of cells at plasmid concentrations between 1.3 and 1.6 μg. The transiently transfected cells infected with *R. montanensis* were then monitored under fluorescent microscopy. Up to 24 hours post infection, loss of FRET was detected in the cell monolayers infected with *R. montanensis*, and transfected with plasmid pCDIC-38 as evidenced by an increase in the cyan emission from the cells upon excitation at 433 nm (top right to left). Increased FRET was observed in cells transfected with plasmid YC2.3 (bottom left to right). Positive (ionomycin added to medium) and negative controls (non-transfected cells, and transfected non-infected cells) were used (not shown).

Figure 11.

T_0 T_1 T_3

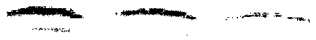

T_0: Immediately following *Rickettsia rickettsii* inoculation.
T_1: One hour after inoculation
T_3: Three hours after inoculation.

THE FASEB JOURNAL

Volume 16, Number 4 March 20, 2002

ABSTRACTS

ASBMB SATELLITE MEETINGS

TRANSCRIPTIONAL REGULATORY MECHANISMS

FRIDAY MORNING
April 19, 2002

FRIDAY AFTERNOON
April 19, 2002

SATURDAY MORNING
April 20, 2002

SATURDAY AFTERNOON
April 20, 2002

FRIDAY/SATURDAY
April 19 - 20, 2002

FRIDAY MORNING
April 19, 2002

SCIENTIFIC AND TECHNICAL CHALLENGES IN THE HUMAN PROTEOME

FRIDAY AFTERNOON
April 19, 2002

SATURDAY MORNING
April 20, 2002

SATURDAY AFTERNOON
April 20, 2002

FRIDAY/SATURDAY
April 19 - 20, 2002

MEETING

SATURDAY MORNING
April 20, 2002

American Society for Investigative Pathology

American Association of Anatomists

SATURDAY AFTERNOON
April 20, 2002

American Society for Biochemistry and Molecular Biology

American Society for Investigative Pathology

180.5

Evidence of calmodulin activation in an in vitro model of rickettsial infection

Juan Pablo Olano, Gary Wen. Pathology, University of Texas Medical Branch, 301 University Blvd. Rt 0747, Galveston, Texas 77555

Ionized calcium plays a pivotal role in the intracellular signal transduction pathways (STP?s) of eukaryotic cells. Calmodulin is an intracellular calcium-binding protein that acts as a transducer of intracellular calcium (Ca[I]) signals mainly through its calcium-dependent activation of different kinases. Calcium-related events after rickettsial internalization are unknown. Previous experiments performed in our laboratory have shown elevation of Ca[I] in mouse endothelial cell monolayers infected with spotted fever group and typhus group rickettsiae. The highest levels were seen at 6 hours after infection. In order to determine whether the observed changes in Ca[I] induce activation of calmodulin, liposome-mediated transfection of COS cells was performed with plasmids pCDIC-38 (Persechini A, et.al.) and YC2.3 (R. Tsien, et.al) containing enhanced cyan and yellow fluorescent protein gene sequences linked by the calmodulin binding site of avian smooth muscle myosin light chain kinase (MLCK) sequence (pCDIC-38) and by fragments of the calmodulin molecule and MLCK (YC2.3). Infected cells revealed loss of fluorescence resonance energy transfer (FRET) with the first plasmid and presence of FRET with the second plasmid, suggesting calmodulin activation.